

Oct. n° 2/3, oct.

[5]

Seismological investigation of the Bangui magnetic anomaly region and its relation to the margin of the Congo craton

Catherine Dorbath^{1,2}, Louis Dorbath^{1,2}, Roland Gaulon² and Denis Hatzfeld³

¹ ORSTOM, 24 rue Bayard, 75008 Paris (France)

² LEGSP, LA 195, CNRS, Laboratoire de Sismologie, IPG, 4, Place Jussieu, 75230 Paris Cedex 05 (France)

³ IRIGM, B.P. 68, 38402 Saint-Martin d'Hères Cedex (France)

Received January 11, 1985; revised version accepted July 8, 1985

Inversion of teleseismic travel times of P-waves recorded by a temporary linear array of seismological stations has been carried out in order to investigate the deep P-wave velocity structure in the Central African Republic in a region where a large magnetic anomaly—one of the largest occurring over a stable continent—has been revealed by satellite and surface surveys. Because of the good azimuthal coverage of seismic sources, it turned out that most of blocks are sampled by rays crossing in widely different directions. Lateral inhomogeneities strongly bias 2-D inversion and explain why 3-D inversion improves the fit of the data. Structural variations persist down to a depth of 160 km. Crustal thickness is about 40 km. Lateral inhomogeneities may be related to the northern margin of the Congo craton where up to 4% higher velocities are observed. The similar patterns of the Bangui magnetic anomaly and of the seismic velocity distribution suggest a close relation between the two. The abnormal magnetic field could be due to a deep structure with a higher susceptibility.

1. Introduction

The Bangui magnetic anomaly was first detected from surface measurements in 1953 [1]. Further observations—aeromagnetic profiles at an altitude of 3 km [2,3] and measurements by satellites Pogo [4,5] and, more recently, Magsat [6]—provide independent evidence for these features (Fig. 1). The latest data confirm that this is one of the largest anomalies detected at the earth's surface in both intensity and dimension. Ground measurements [7] show finer structures with three abnormal areas: the largest intensity is found north of Grimari (−1500 nT), the second zone is northwest of Bangui, between Bangui and Bossembele (−600 nT) and it is at the same location as the low of the satellite values. The third one is centered south of the Bossangoa region (−400 nT); this area may be related to the massive outcrops of charnockite [8].

Interpretation of aeromagnetic profiles led Green [3] to propose a crustal origin for the anomaly. According to Han-Shou-Liu [9] the

source would be a remanent magnetization due to compressional stresses within the crust. On the other hand, Regan and Marsh [10] indicated that induced crustal sources could explain most of the observations. Galdeano [11] showed that the direction of the magnetization is the same as the present field after reduction to the pole; he also noted that, in the reconstruction of the Gondwana continent, there is a noteworthy continuity of anomalies between Africa and South America. These observations all support an induced magnetization.

The anomaly is thus the result of the present earth's magnetic field acting on a body whose susceptibility is larger than that of the surrounding regions. This body can extend as far as the depth related to the Curie isotherm so that it could extend as deep as the bottom of the crust or perhaps into the upper mantle. Moreover, this anomaly is not connected in a very clear way with surface geology. Gravity data also exhibit anomalous features. The Bouguer anomaly map delineated by Albouy and Godivier [12] clearly indicates a gravity low with an amplitude of 50 mgal with respect to surrounding regions at about the

Contribution IPG No. 863.

0012-821X/85/\$03.30 © 1985 Elsevier Science Publishers B.V.

13 MAI 1986

O. R. S. T. O. M. Fonds Documentaire

N° : 27 027 155

Cote : B. 21.027

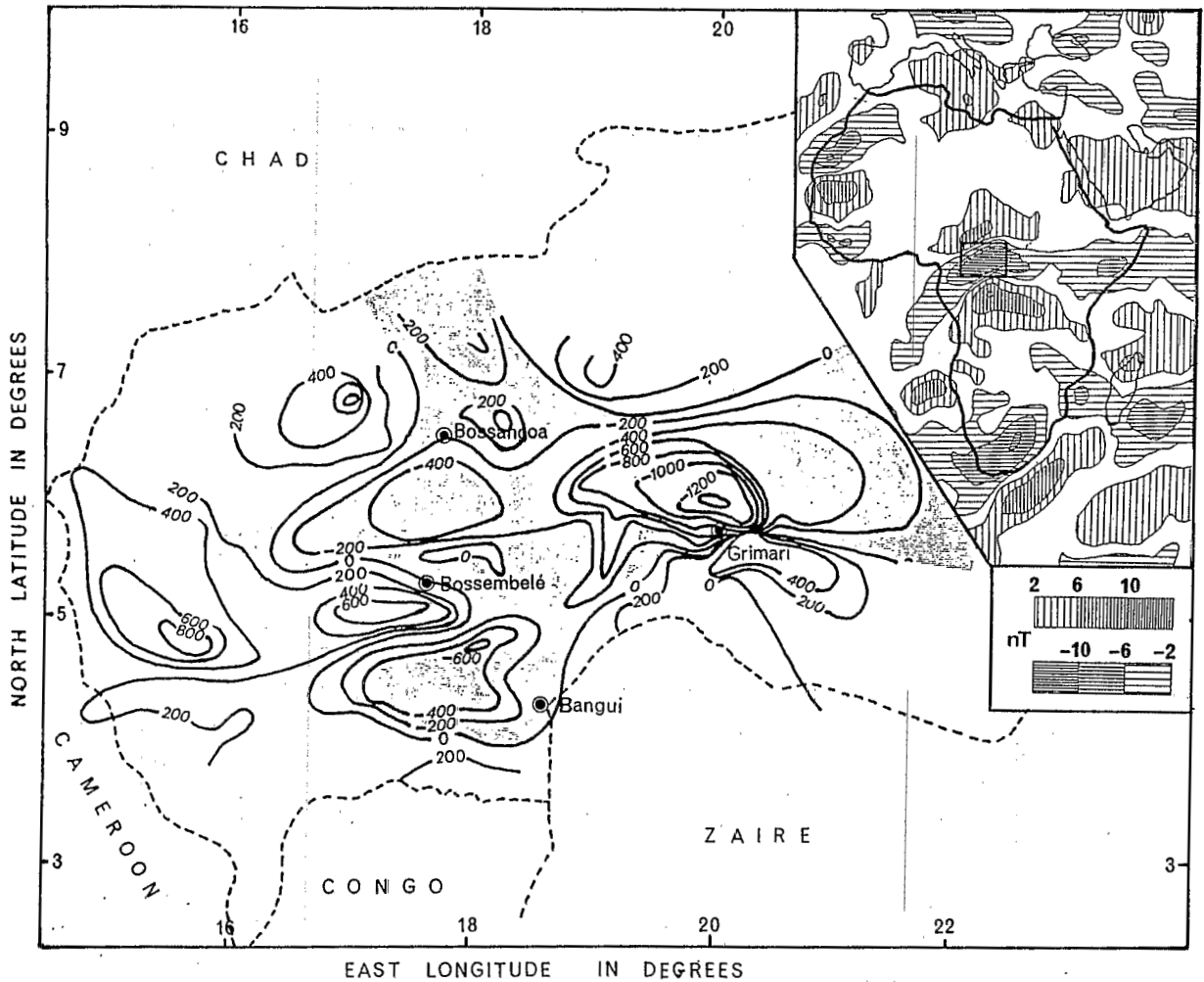


Fig. 1. Total magnetic field anomaly in Central African Republic from ground measurements after Vassal and Godivier [7]. Contour interval is 200 nT. In inset, total magnetic field anomaly in Africa from Magsat after Langel et al. [30]. Contour interval is 4 nT.

same location as the magnetic anomaly. However, this gravity low may not have a deep origin, since it is partly related to the sedimentary series of Bangui-Mbaiki to the west, and northwest of Bangui to the Ubangian series and to the granitic intrusions that cut them in the area of Sibut, Grimari and Bambari. Regan and Marsh [10] presented a model explaining the gravimetric and long-wave length magnetic observations. They attempted to satisfy these data only with crustal inhomogeneities. Their model consists of an intrusive body with its top at a depth of 3 km and its base at about 35 km; the susceptibility reaches 10^{-2} cgs. This body is covered with a quartzite

sedimentary series of low susceptibility and is surrounded by charnockites of higher susceptibility.

Most of the Central African Republic is late Precambrian in age, except for the Mesozoic sandstone at Carnot in the far east and several alluvial formations along the rivers. The large extension of the sandstone quartzite shale series is seen in Fig. 2. It represents a small part of the Lindian-Ubangian rocks formed in much of North Zaire. They are typical of shallow marine deposits. These series have a stronger continental type here. The Lindian-Ubangian rocks represent the lid of an old platform (Congo craton) according to Verbeek [13], so that the Bangui-Mbaiki series would have

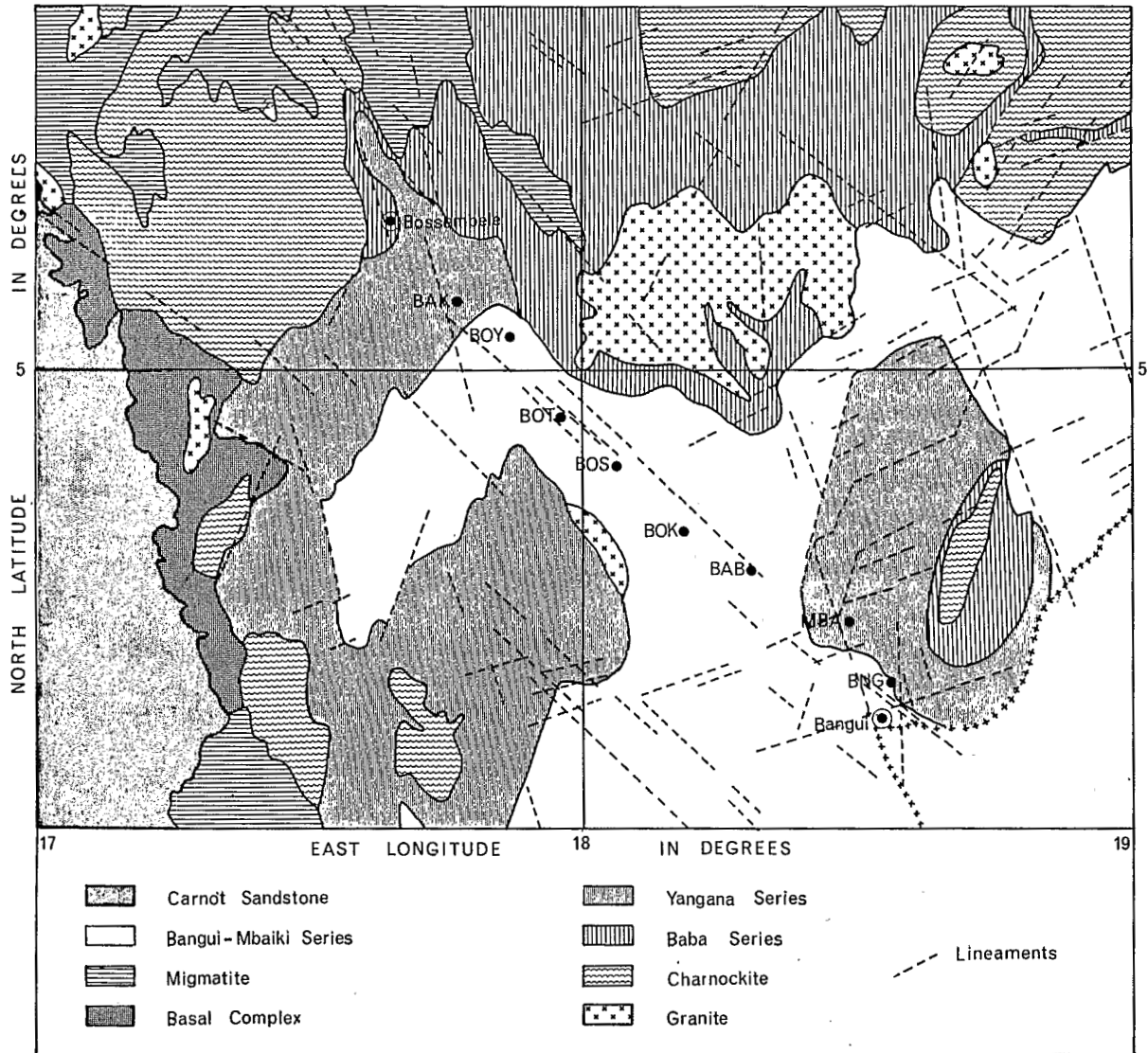


Fig. 2. Geological map of the Bangui area (after Labrousse [31]) and locations of the seismological stations.

been altered by the Pan-African orogeny [14]. The mica-schist and sandstone formations, which encircle the craton, consist of older series among the other metamorphic formations. The main structural rocks strike NNW and from WSW to ENE.

It seems that the area has not been tectonically active since the end of the Precambrian times and beginning of Paleozoic era (Pan-African episod). Nevertheless several small earthquakes have been felt in the last few years (Boali, 1967 and 1972; Yaloke, 1974; Bangui, 1976; Bossembelé, 1979), comparable to the seismicity reported around old stable areas [15].

2. Data

In order to study the velocity structure within the crust and upper mantle, we installed 8 Sprengnether smoked-paper recorders along a linear profile from Bangui to Bossembelé across the maximum of the magnetic anomaly, the average distance between stations being 15–20 km (Fig. 2). The field experiment lasted two and a half months from mid December 1980 to early March 1981. The high quality of the sites permitted a gain up to 90 db. The internal clock shift was controlled by

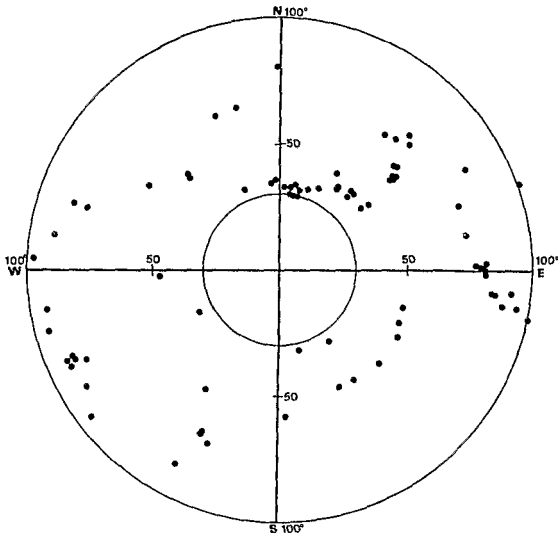


Fig. 3. Plot of the epicenters of the events used in this study as a linear function of distance and azimuth.

daily recording of WWV signals and was smaller than 0.1 s/day.

About 300 events were collected during the ten weeks. The recording speed (120 mm/mn), sharpness of smoked-paper lines, time marks each second and careful reading with micrometric lens allowed us to pick the time with an accuracy of 0.025 s. Each P or PKIKP phase was independently read by two persons and kept if the difference was smaller than 0.15 s. We kept events recorded by more than six of the eight stations with epicentral distances greater than 30° for P-waves. We did not keep PKIKP travel times for distances between 137° and 150° to prevent misreadings of forerunners of triplicated core-phases. The final data set included 930 travel times from 129 events, 98 with epicentral distances, Δ , in the range 30 – 100° and 31 with Δ greater than 110° . 30% of the data showed differences in double reading smaller than 0.05 s and their standard deviation may be assessed less than 0.1 s.

Events used in this study are plotted in Fig. 3. Azimuthal coverage and distance distribution are fairly good, but, for a given azimuth, distances do not vary in a large range due to the world seismicity distribution.

In order to eliminate source and upper mantle propagation effects, residuals were calculated by the following procedure. Given an event i reported

by station j , the absolute residual is:

$$R_{ij} = (T_{ij} - T_{i0}) - C_{ij}$$

where T_{ij} = observed arrival time, T_{i0} = origin time for event i , and C_{ij} = computed travel time for this hypocenter.

The data were corrected for ellipticity and elevation. Residuals were calculated using the Jeffreys-Bullen tables.

R_{ij} is affected by various errors and anomalies including event mislocation and model biases. To take into account only the effects beneath the network of stations, we calculated the relative residuals r_{ij} :

$$r_{ij} = R_{ij} - R_i$$

where mean residual R_i for event i is the arithmetic mean of R_{ij} :

$$R_i = \left(\sum_{j=1}^{n_i} R_{ij} \right) / n_i$$

where n_i = number of stations reporting the P arrival for event i .

Finally, the mean station residual r_j was calculated for station j :

$$r_j = \left(\sum_{i=1}^{n_j} r_{ij} \right) / n_j$$

TABLE 1

Summary of P- and PKIKP-wave residuals

Station	r	σ	n
<i>(a) P-wave data</i>			
BNG	-0.13	0.16	88
MBA	-0.16	0.11	89
BAB	-0.07	0.10	86
BOK	-0.03	0.10	83
BOS	-0.03	0.09	89
BOT	0.05	0.10	93
BOY	0.14	0.12	89
BAK	0.24	0.13	83
<i>(b) PKIKP-wave data</i>			
BNG	-0.09	0.10	28
MBA	-0.11	0.07	27
BAB	-0.01	0.08	28
BOK	0.05	0.09	26
BOS	0.01	0.07	28
BOT	0.04	0.07	29
BOY	0.02	0.10	25
BAK	0.14	0.09	17

r = mean station residual, σ = standard deviation, and n = number of events.

where n_j = number of events observed at station j .

R_j will include travel-time errors due to mislocation and long-wave length inhomogeneities in the source region and in the lower mantle which are assumed to affect all stations similarly.

(1) We checked that *absolute residuals*, R_j , as a function of distance are similar to those generally observed ([16,17], for example), and thus not due to the local structure anomaly. Therefore there should be no major bias introduced by this reduction.

(2) *Mean station residuals*, r_j , are listed in Table 1a with standard deviation and number of events. Earliest arrivals are observed at the southeastern end of the array (BNG and MBA) and the latest ones at the northwest (BOY and BAK), the difference amounting up to 0.4 s. Velocities are therefore higher in the southeast than in the northwest. Variations are not regular: the values increase

more rapidly between BNG and BAB than between BOT and BAK (0.1 s between two neighboring stations). The standard deviation is larger at the ends than in the middle of the array. This may be explained by azimuthal variations with larger amplitudes as we shall see later. Mean station residuals for PKIKP phases have also been calculated (Table 1b). Residuals and standard deviations are smaller in absolute values for rays emerging more vertically and, consequently, less perturbed by lateral inhomogeneities. However, the azimuthal coverage is not as good as that of the P phases: more than 70% of the observed PKIKP rays have azimuths between 90° and 150° and the variations of P-wave relative residuals along the profile are weaker in this direction. This fact may explain the differences between P and PKIKP values.

(3) *Relative residuals*, r_{ij} , as a function of azimuth are shown in Fig. 4. At BNG (Bangui) a

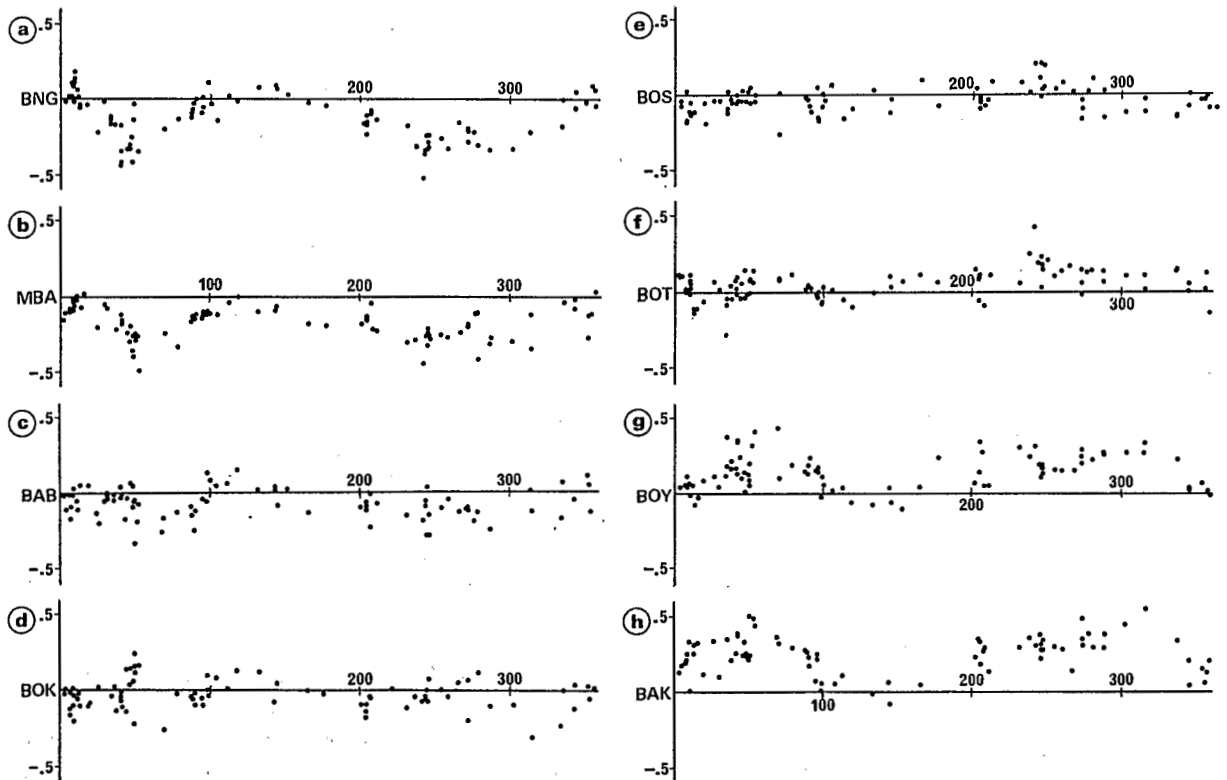


Fig. 4. Relative residuals as a function of azimuth for each station. There is a distinct variation of opposite sign at both ends of the profile (stations BNG, MBA in the southeast and stations BOY and BAK in the northwest) but not in the middle of the profile (stations BOS and BOT).

double swing is seen with lower values at about 50° and $250\text{--}300^\circ$ and higher values at 0° and 140° . Amplitude of the variations is about 0.4 s. The next station MBA shows the same pattern but with a smaller amplitude, and a negative offset, and therefore, the mean residual is more negative here than at BNG. Such a situation is still observed at BAB, again with a very small amplitude (about 0.2 s). The three following stations (BOK, BOS and BOT) do not show a clear azimuthal variation. For the two last stations (BOY and BAK) a clear variation is seen again, but contrary to the first stations, peaks are observed at 50° and $250\text{--}300^\circ$ and troughs at 0° and 130° ; amplitude is about 0.4 s. If we try to explain all these observations of residuals r_{ij} by variations in the thickness of the crust or in crustal velocities, we have to use models dipping more than 30° or having unreasonable velocities. Thus we have to look for inhomogeneities within the upper mantle. Attempts have been made to set up simple two-dimensional models of two or three blocks centered below the array; this was unsuccessful since we could not obtain the observed azimuthal distribution of residuals.

To summarize the observations and preliminary results:

—Variations of the station mean residuals r_i up to 0.4 s along the profile may correspond to an increase of 2.5 km in crustal thickness or to a 6% decrease in average crustal velocity, from the southeast to the northeast.

—The azimuthal variations for residuals r_{ij} will not be explained in this manner and lateral inhomogeneities are necessary to fit residual data in azimuth and in amplitude.

—Reading errors (0.1 s) can explain less than 30% of variance of the data ($3 \times 10^{-2} \text{ s}^2$). Therefore lateral inhomogeneities have to account for 70% of this variance, and thus we have to try an inversion of the velocity structure beneath the network.

3. Inversion

As a model for the structure beneath the array we shall use a stack of rectangular homogeneous blocks. Aki et al. [18] and Aki and Richards [19] have shown that the vector m of the perturbations of the P-wave velocity is a solution of the equa-

tion:

$$Gm = d$$

where d is the vector of relative residuals of P-wave arrivals, m , the vector of unknown velocity perturbations, and G , a matrix with reduced travel times.

Selection of an initial model requires a reasonable knowledge of the vertical velocity distribution, because perturbations are not linearly related to the observations. Estimations of the crustal thickness and velocity can be found by calculating spectral ratios of horizontal and vertical amplitudes of the P-waves at the S.R.O. station at Bangui (Table 2) according to the method of Phinney [20]. We tried to fit these spectral ratio with different crustal models. Solutions are not unique and peak positions depend on the travel time within the crust, thence on crustal thickness and velocity (Fig. 5). This thickness ranges from 36 to 42 km as the P-wave velocity varies from 6.1 to 6.7 km/s. A shot of 350 kg TNT in a quarry near Bangui provides arrival times compatible with this crustal model. We tried several initial models taking into account these results and different upper mantle velocity distributions ([21], PEM [22], AFRIC [23]), but the solution does not drastically depend on a specific model and we selected the model of Herrin in the following.

The block size that needs to be chosen is related to wavelength, angles of incidence, distance and azimuth of rays and also to the geometry of the network, and is controlled by the usual trade-off between resolution or details of models and accuracy of the model parameters. The number of blocks and their horizontal size are fixed in the first layer by the station distribution and they have not been perturbed for the different trials. Rotation of the blocks did not modify the obtained solution significantly and increasing the block size spreads the resolution, but does not change the pattern drastically.

The damping constant $\theta^2 = \sigma_n^2 / \sigma_m^2$ of the stochastic inverse solution [24,25]— σ_n is the standard deviation of data and σ_m that of the model—may be calculated a priori and we reported before that σ_n^2 was $3 \times 10^{-2} \text{ s}^2$. A reasonable estimate of σ_m^2 may be $20(\%)^2$. We tried several values of θ^2 between 0.0001 and $0.015 (\text{s}/\%)^2$. Higher values of θ^2 reduce the number of degrees of freedom,

TABLE 2

Parameters of the events used in Fig. 5

Catalog No	Date	Time	Location	Magnitude m_b (U.S.G.S.)
306	11/02/1979	15 53 03.5	7.656°S, 108.252°W	6.1
326	11/22/1979	02 41 16.7	24.344°S, 67.385°W	5.8
327	11/23/1979	23 40 29.8	4.805°S, 76.217°W	6.4

therefore the perturbation reveals large-scale anomalies, while lower values have the effect of increasing small-scale fluctuations. A fair trade-off is obtained with a value of $0.001 (s/\%)^2$.

Because the network was linear, we began with looking for two-dimensional models: the block size is largely increased perpendicularly to the profile. We could not obtain models that reduce the variance of the data by more than 64%. However, we previously stated that we had to justify 70% at least.

Data from a field experiment in Senegal [26], performed in very similar conditions, have been reprocessed using the same technique as applied here [27]. We found that most of the data could be explained with a two-dimensional model. Indeed, in that case the geological settings show a clear structural trend perpendicular to the profile which explains the success of the 2-D inversion.

Our best 2-D model (Fig. 6a) reveals a rather simple structure: the first 3 layers show higher velocity in the southeast and lower velocity in the northwest and overlay a homogeneous half-space.

For such a simple model we expect that the azimuthal variations of residuals at the stations BOS and BOT located near the boundary between regions of higher and lower velocities would be very much larger than those at both ends of the profile. However, we see in the Fig. 4e and 4f that the azimuthal variations are in fact smaller for these stations compared with the two ends of the profile. Therefore this model cannot explain these residuals; we found the same result when we tried to look for a velocity perturbation only within the crust. If the 2-D model cannot explain the variance in the data then lateral inhomogeneities must exist perpendicular to the trend of the array.

The quality of the data is comparable to that in

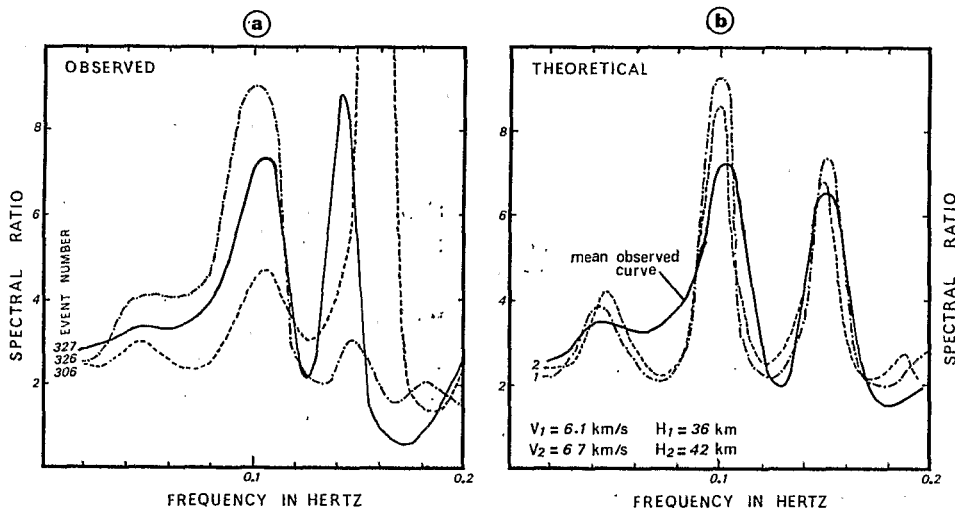
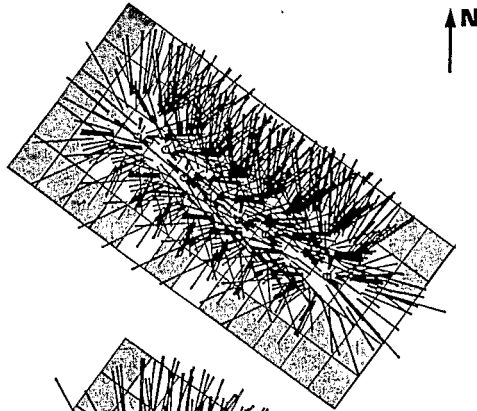
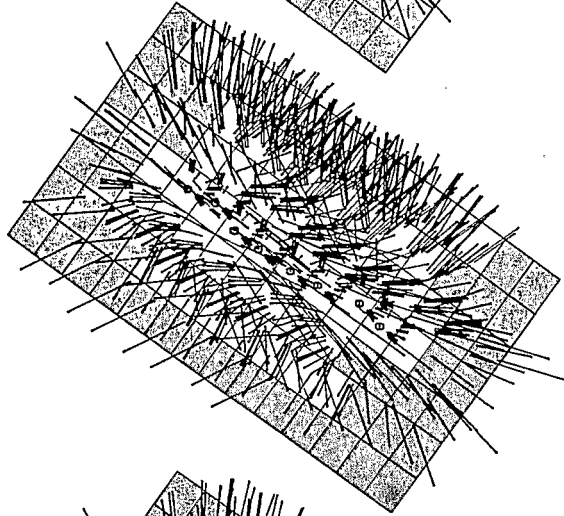


Fig. 5. Spectrum ratio of horizontal and vertical components of P-waves recorded at S.R.O. station BCAA (Bangui). (a) Observed spectrum for 3 events (event number listed in Table 2). (b) Theoretical spectrum for a homogeneous crust. Thickness: 1 = 36 km; 2 = 42 km; velocity: 1 = 6.1 km/s; 2 = 6.7 km/s. Note the trade-off between thickness and velocity of the two extreme solutions.

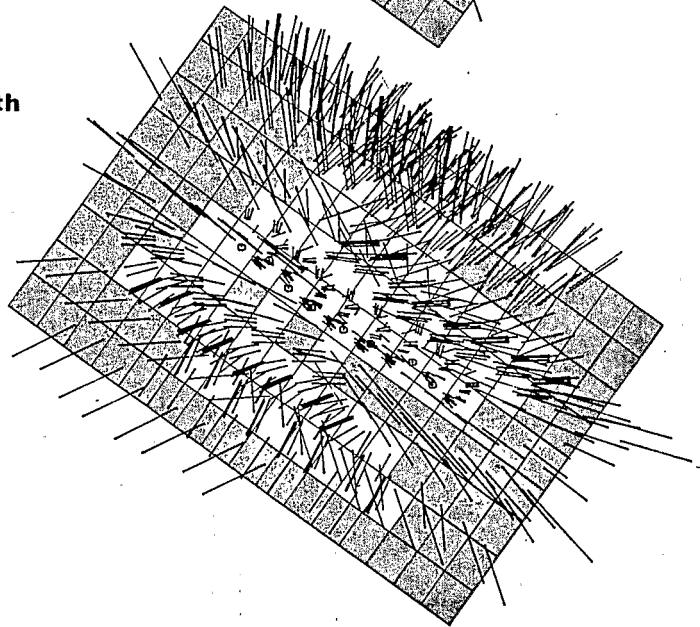
Layer 3
40-80 km depth



Layer 4
80-120 km depth



Layer 5
120-160 km depth



50 km

Fig. 7. Horizontal projection of the ray paths in three layers. Note the wide coverage of azimuth in each resolved block. The shaded blocks are not well resolved. Open circles are the stations.

The result of this inversion is represented in Fig. 6b. It is seen that the model now explains 72% of the variance of the data; it is quite different

from the 2-D solution indicating how much the first inversion was biased.

Next, we consider an elongated 3-D model and

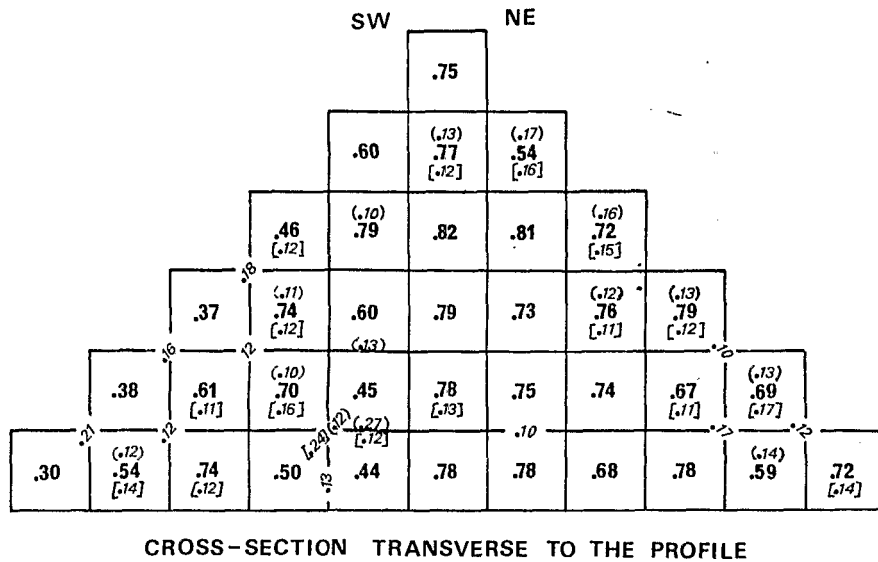


Fig. 8. Values of the elements of the resolution matrix for blocks in a vertical cross-section transverse to the 3-D model. Bold characters inside each block indicate the value of the diagonal element of the resolution matrix for this block. Italicized characters represent off-diagonal elements of this matrix corresponding to neighbouring blocks. Only off-diagonal elements greater than 0.10 are presented. Note that the distribution of off-diagonal elements is isotropic for well-resolved blocks (diagonal element of the resolution matrix greater than 0.50). () = block in front; [] = block behind.

compare its vertical section along the profile with that of the unbiased 2-D inversion in order to control the stability of the inversion process. 70% of the variance of data are explained with a simple model consisting of 2 layers, 80 km thick. This model is compatible again with the unbiased solution. We shall perturb this new model further by building up a stack of layers extending down as deep as 160 km. Beyond a depth of 160 km, most of the blocks are not resolved. It is clear that there is no resolution near the surface for off-line elements and that resolution increases in depth with the number of rays crossing within these blocks like for the on-line parts.

Our best model is listed in Table 3. It consists of six layers with two blocks within the crust and it explains 85% of the data variance. The magnitude of remaining residuals (0.07 s) is in agreement with the errors estimated previously.

The vertical section (Fig. 6c) along the array is comparable to that of the 2-D unbiased model. This result indicates that the 3-D inversion is stable. Therefore we shall discuss this model further later on.

Horizontal projection of the ray paths through each block of three layers of the model are shown

in Fig. 7. This figure allows us to understand how the 3-D inversion of the data of a linear array may be successful. Neighboring resolved blocks do not share the same rays, but are sampled by rays coming from various directions or distances. This is due to the good azimuthal coverage of the different seismic sources (see Fig. 3). If the number of rays crossing through a block and coming from different source regions becomes small (generally less than 10), then this block is found unresolved in the model.

Another verification of the 3-D resolution can be found by looking at the off-diagonal elements of the resolution matrix. Fig. 8 shows the values of these elements for a vertical section transverse to the profile. The figure indicates that the values for each resolved block are not greater in roughly vertical directions as would be the case if there was a strong correlation along the rays, but it shows more or less isotropic variations.

4. 3-D velocity model

The final solution is shown in Fig. 9 where the velocity values are indicated only for blocks with the R_{ii} component of the resolution matrix greater

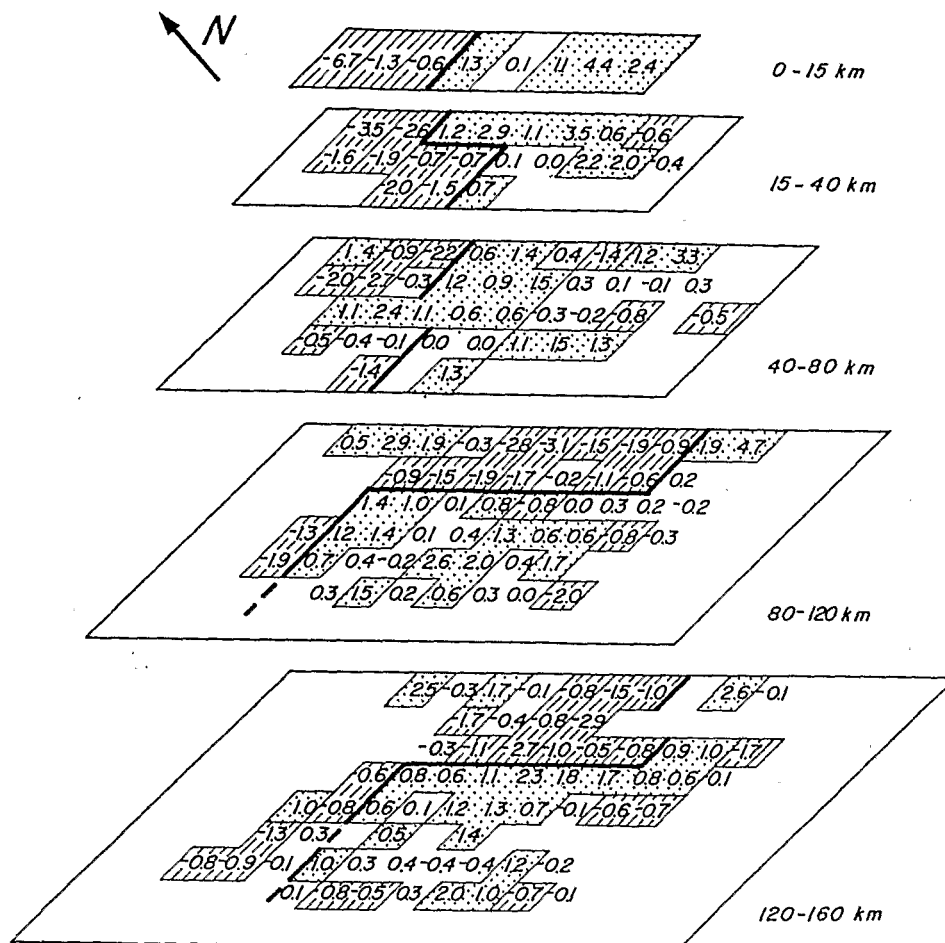


Fig. 9. Three-dimensional model of P-wave velocity beneath the Bangui magnetic anomaly area. Velocity anomalies are given in percent of P-wave velocity in the layer. Dots indicate positive anomalies and oblique hatchings correspond to negative ones for the blocks with velocity perturbations higher than 0.5%, in absolute value.

than 0.5. For the contributing blocks the standard deviation is about 0.5–0.6%.

The three first layers have similar patterns extending down to a depth of 80 km: higher velocities are seen in the southeast, lower ones in the northwest. The greatest fluctuations are found in the shallower layers where they reach 10% and they are slightly larger than perturbations necessary to explain mean station residuals by assuming velocity variation only within the crust. In the second layer (15–40 km) there is some evidence of lower velocities in the southeastern edge. This trend will be strengthened in deeper layers. The negative magnetic anomalies are located at the same place as the high crustal velocities that are

observed in the southeast.

Variations of Bouguer and velocity anomalies have an unusual relationship: higher velocities are associated with the most negative gravity values and vice versa, but it may be that Bouguer data depend on shallow structures as suggested before [10].

In layers 4 (80–120 km) and 5 (120–160 km) large-scale heterogeneities are found extending within both levels. A higher-velocity body is visible in the middle and in the southwest edge of the model. It is bounded by lower-velocity areas, more sharply in the northwest, where contrasts exceed 3%, than in the southeast, where they are found to be about 1% as already observed in the

TABLE 3
Characteristics of the 3-D velocity model

Layer No.	Velocity	Thickness	N_{\perp}	L_{\perp}	N_{\parallel}	L_{\parallel}	M
1	6.00	15	1	20	8	16.5	8
2	6.75	25	3	20	10	16.5	30
3	8.07	40	5	20	12	16.5	60
4	8.11	40	7	20	14	16.5	98
5	8.17	40	9	20	16	16.5	144
6	8.25	40	11	20	18	16.5	198

N_{\perp} , L_{\perp} = number, length of blocks in a direction perpendicular to the profile; N_{\parallel} , L_{\parallel} = number, length of blocks in a direction parallel. M = number of blocks in the layer.

second layer. Boundaries between fast and slow regions strike roughly perpendicular to the profile. In the northeast a wide region of lower velocity appears which was not observed in the three first layers. Perhaps this feature may extend upwards, but the absence of off-line resolution in these three layers does not permit to reveal it.

Below 160 km low velocities continue to be observed in the northeast, but inhomogeneities are of a smaller scale. There is no more lateral resolution.

In conclusion, the three-dimensional travel-time inversion illustrates that differences in structure extend down to 160 km and may be deeper. A high-velocity body is clearly indicated with a sharp boundary to the northeast. The geometry of the network prevents us from knowing if this pattern extends up to the surface. If this is the case, the fast region would roughly consist of a sort of wedge with sides striking respectively SW-NE and NW-SE, the first one dipping steeply toward the northwest and the other one subvertically.

5. Discussion

The location of the northern boundary of the Congo craton is still an open problem. In Cameroon the limit to the west is well determined until 14–16°E and in the Central African Republic and in Zaire it is found again for longitudes greater than 22°E. Bessolles and Trompette [14] and Cornacchia and Dars [28] do not agree upon the latitude which may vary up to several tens of kilometers: between 2° and 4°N for the eastern

end in Cameroon and between 4° and 5°N at longitude 22°E, northwards according to Cornacchia and Dars, southwards according to Bessolles and Trompette. Between 14–16°E and 22°E radiometric datings are poor markers of the craton and the Pan-African mobile zone. The margin could be hidden under upper Precambrian series which may not have clear characteristics allowing to assert that these series are cratonic coverage.

Poidevin [29] from new geological observations showed that this margin of the Congo craton is characterized by a suture which presents a sequence of sinistral offsets approximatively striking N020°. One of the edges defined by these offsets, northwest of Bangui, roughly coincides in location with the high-velocity zone revealed by the inversion. Therefore these deep P-waves velocity inhomogeneities could be related to the Congo craton or to some old suture in its surroundings.

Moreover, Poupinet [17] showed a close relation between P-wave residuals and ages of the underlying lithosphere. He found a mean residual of -1.36 s, corresponding to an age of 3 Ga at Bangui station. In this case this station would be located on the craton, whereas Bessolles and Trompette [14] think that the whole Central African Republic belongs to the Pan-African mobile zone. We operated a temporary seismological station during several days, 20 km west from Bossembelé, 40 km west from the northwestern end of the profile. Compared to BNG a mean differential residual of 0.64 ± 0.14 s has been calculated based on only 11 events. In this case absolute residuals would be about -0.72 s and the underlying lithosphere would be about 1 Ga old. We think that the northern margin of the Congo craton is located between the extremities of the profile.

Looking again at the magnetic map from surface measurements (Fig. 1), it is seen that the low magnetic anomaly spreads widely towards the southeast and terminates to the northwest along an ESE/WNW direction crossing the seismological station profile and also, in a less clear evidence, to the northeast of the network. Both anomalies are therefore characterized by a similar wedge shape with sides trending parallel to both main structural directions in this region, just at the place where the boundary of the craton may be located. If a geometrical relation between structural and magnetic anomaly looks fairly well established, we

did not establish how this structure may induce the observed magnetic field. We did not try to build up a model of an induced magnetic anomaly because of the poor constraints that we would be able to introduce: lateral extensions southwards and also upwards in the first layers are not defined by our data. Moreover, large variations of the Curie isotherm depth may be considered. Further constraints must be introduced, but this investigation is beyond the range of this paper.

6. Conclusion

A seismological investigation of the large magnetic anomaly near Bangui suggests interesting structural differences extending as deep as 160 km. Even though local conditions forced us to set up only a linear profile 120 km long, the observed data can only be explained with lateral inhomogeneities that are both longitudinal and transverse to the profile. The exceptional quality of the sites made it possible to consider observations from sources differing in epicentral distance and azimuth and this good azimuthal coverage indicates that most blocks are sampled by rays pathing through them in different directions. Two-dimensional inversion is strongly biased.

The three-dimensional inversion suggests the existence of a fast-velocity wedge in the southwest of the investigated region which may belong to the northern margin of the Congo craton. In this southwest region the magnetic field and the velocity distribution have a similar wedge-like shape which led us to put forward the hypothesis that the magnetic anomaly and the higher velocities reveal a common abnormal structure. The magnetic anomaly would be related to a body of high magnetic susceptibility and higher seismic velocities.

References

- 1 R. Godivier and L. Le Donche, Réseau magnétique ramené au 1er Janvier 1956: République Centrafricaine, Tchad Méridional, ORSTOM, Paris, 1956.
- 2 H.P. Stockard, Worldwide surveys by project Magnet, World magnetic survey, 1957-1969, Int. Assoc. Geomagn. Aeron. Bull. 28, 60-64, 1971.
- 3 A.G. Green, Interpretation of project Magnet aeromagnetic profiles across Africa, Geophys. J. R. Astron. Soc. 44, 203-228, 1976.
- 4 R.D. Regan, W.M. Davis and J.C. Cain, The Bangui magnetic anomaly (abstract), EOS, Trans. AGU 54, 236, 1973.
- 5 R.D. Regan, J.C. Cain and W.M. Davis, A global magnetic anomaly map, J. Geophys. Res. 80, 794-802, 1975.
- 6 R.A. Langel, Satellite magnetic anomaly maps, EOS, Trans. AGU 62, 269, 1981.
- 7 J. Vassal and R. Godivier, Anomalie magnétique en Centrafrique, un modèle géophysique, 10 pp., ORSTOM, Paris, 1979.
- 8 G. Pouit, Etude Géologique des Déformations métamorphiques granitiques et charnockites de la région de Fort-Crampel (Oubangui-Chari), Thèse Univ. Dir. Mines Geol. A.E.F., 13, 1959.
- 9 Han-Shou-Liu, Convection pattern and stress system under the African plate, Phys. Earth Planet. Inter. 15, 60-69, 1977.
- 10 R.D. Regan and B.D. Marsh, The Bangui magnetic anomaly: its geological origin, J. Geophys. Res. 87, 1107-1120, 1982.
- 11 A. Galdeano, Les mesures magnétiques du satellite Magsat et la dérive des continents, C.R. Acad. Sci. Paris, II, 293, 161-164, 1981.
- 12 Y. Albouy and R. Godivier, Cartes gravimétriques de la République Centrafricaine, 8 pp., ORSTOM, Paris, 1981.
- 13 T. Verbeek, Géologie et lithologie du Lindien (Précambrien supérieur du nord de la République Démocratique du Congo) Mus. R. Afr. Centr., Tervuren, An. Ser. Sci. Geol. 66, 311 pp., 1970.
- 14 B. Bessolles and R. Trompette, Géologie de l'Afrique. La chaîne panafricaine (zone mobile d'Afrique Centrale (partie sud et zone mobile Soudanaise), Mem. BRGM 92, 396 pp., 1980.
- 15 S.G. Wesnouski and C.H. Scholz, The craton: its effect on the distribution of seismicity and stress in North America, Earth Planet. Sci. Lett. 48, 348-355, 1980.
- 16 B.R. Julian and M.K. Sengupta, Seismic travel time evidence for lateral inhomogeneities in the deep mantle, Nature 242, 443-447, 1973.
- 17 G. Poupinet, Hétérogénéités du manteau terrestre déduites de la propagation des ondes de volume: Interprétation géodynamique, 234 pp., Thèse Univ. Sci. et Med., Grenoble, 1977.
- 18 K. Aki, A. Christofferson and E.S. Husebye, Three dimensional seismic structure of the lithosphere under Montana Lasa, Bull. Seismol. Soc. Am. 66, 501-524, 1976.
- 19 K. Aki and P.G. Richards Quantitative Seismology—Theory and Methods, Vol. 2, W.H. Freeman and Co., San Francisco, Calif., 1980.
- 20 R.A. Phinney, Structure of the Earth crust from spectral behaviour of long period body waves, J. Geophys. Res. 69, 2997-3017, 1964.
- 21 E. Herrin, Seismological tables for P phases, Bull. Seismol. Soc. Am. 58, 1193-1421, 1968.
- 22 A. Dziewonski, A. Hales and E. Lapwood, Parametrically simple Earth models consistent with geophysical data, Phys. Earth Planet. Inter. 10, 12-48, 1975.
- 23 F. Gumper, and P.W. Pomeroy, Seismic wave velocities and Earth structure on the African Continent, Bull. Seismol. Soc. Am. 60, 651-668, 1970.
- 24 W.L. Ellsworth, Three-dimensional structure of the crust and mantle beneath the Island of Hawaii, 327 pp., Ph.D. Thesis, MIT, 1977.

- 25 J.N. Franklin, Well-posed stochastic extension of ill-posed linear problems, *J. Math. Anal. Appl.* 21, 682-716, 1970.
- 26 J.C. Briden, D.N. Whitcombe, G.W. Stuart, J.D. Fairhead, C. Dorbath and L. Dorbath, *Nature* 292, 123-128, 1981.
- 27 C. Dorbath, L. Dorbath, A. Le Page and R. Gaulon, The West African craton margin in eastern Senegal: a seismological study, *Ann. Geophys.* 1 (1), 25-36, 1983.
- 28 M. Cornacchia and R. Dars, Une ligne structurale majeure du continent Africain, *Bull. Soc. Geol. Fr., Sér. 7, A*, XXXV/1, 101-109, 1983.
- 29 J.L. Poidevin, Le Protérozoïque supérieur de la République Centrafricaine. Stratigraphie et structures (in preparation).
- 30 R.A. Langel, J.D. Philips and R.J. Horner, Initial scalar magnetic anomaly map from Magsat, *Geophys. Res. Lett.* 9, 269-272, 1982.
- 31 B. Labrousse, Etude structurale et géologique de l'Empire Centrafricain, 85 pp, ORSTOM, Bangui, 1978.